

An Ultrasonic Strain Gauge

Mathias Kersemans, Klaas Allaer, Joris Degrieck, Koen Van den Abeele,
Lincy Pyl, Filip Zastavnik, Hugo Sol, Wim Van Paegem

► **To cite this version:**

Mathias Kersemans, Klaas Allaer, Joris Degrieck, Koen Van den Abeele, Lincy Pyl, et al.. An Ultrasonic Strain Gauge. Le Cam, Vincent and Mevel, Laurent and Schoefs, Franck. EWSHM - 7th European Workshop on Structural Health Monitoring, Jul 2014, Nantes, France. 2014. <hal-01022047>

HAL Id: hal-01022047

<https://hal.inria.fr/hal-01022047>

Submitted on 10 Jul 2014

HAL is a multi-disciplinary open access archive for the deposit and dissemination of scientific research documents, whether they are published or not. The documents may come from teaching and research institutions in France or abroad, or from public or private research centers.

L'archive ouverte pluridisciplinaire **HAL**, est destinée au dépôt et à la diffusion de documents scientifiques de niveau recherche, publiés ou non, émanant des établissements d'enseignement et de recherche français ou étrangers, des laboratoires publics ou privés.

AN ULTRASONIC STRAIN GAUGE

Mathias Kersemans¹, Klaas Allaer¹, Joris Degrieck¹, Koen Van Den Abeele², Lincy Pyl³, Filip Zastavnik³, Hugo Sol³, Wim Van Paepegem¹

¹ Department of Materials Science and Engineering, Ghent University, Technologiepark-Zwijnaarde 903, 9052 Zwijnaarde, Belgium

² Department of Physics, Catholic University of Leuven - KULAK, Etienne-Sabbelaan 52, 8500 Kortrijk, Belgium

³ Department Mechanics of Materials and Constructions, Vrije Universiteit Brussel, Pleinlaan 2, 1050 Brussels, Belgium

Mathias.Kersemans@UGent.be, MathiasKersemans@hotmail.com

ABSTRACT

A method is introduced for the measurements of strain exploiting the interaction between ultrasound waves and characteristics of the insonified specimen. First, the response of obliquely incident harmonic waves to a deterministic surface roughness is utilized. Analysis of backscattered amplitudes in Bragg diffraction geometry then yields a measure for the in-plane strain field by mapping any shift in angular dependency. Secondly, the analysis of the reflection characteristics of normal incidence pulsed waves in frequency domain provides the out-of-plane normal strain field component, simply by tracking any change in the stimulation condition for a thickness resonance. As such, the developed method yields an absolute, contactless and single-sided mapping of a local 3D strain field, in which both sample preparation and alignment procedure are ubiquitous. The ultrasonic strain gauge is applicable to any material, though under the restriction that a deterministic surface roughness is present. Results are presented for cold-rolled DC06 steel samples onto which skin passing of the work rolls is applied. The samples have been mechanically loaded, introducing plastic strain levels ranging from 2% to 35%. The ultrasonically measured strains have been validated with other strain measurement techniques, yielding good agreement. As the ultrasonic strain gauge provides all three strain field components, we extracted Lankford ratios for the DC06 steel sheet at different applied plastic strain levels revealing a strain dependent plastic anisotropy of the DC06 steel.

KEYWORDS : *ultrasound, 3D strain field, DC06 steel, Lankford parameter*

1 INTRODUCTION

A lot of engineering structures, such as large diameter pipelines, are subject to extreme loading conditions during their lifetime, resulting to large (plastic) strains. Assessment of a strain field is crucial in order to ensure the designed functionality of the structure. In practice however, conventional strain measurement techniques are most of the time not applicable in a real industrial environment because of a number of reasons including (i) the need for a reference measurement, (ii) the necessity to physically attach the gauge, (iii) the limited range of measurable strain fields, (iv) the inapplicability for offshore applications and (v) the large sensitivity to small misalignments and external vibrations.

Recently, it has been shown by the present authors that the in-plane parameters of a periodic (sub)surface structure, i.e. periodicities and symmetry orientations, can be ultrasonically characterized in the Bragg scattering regime [1], simply by evaluating the backscattered wave amplitude for a wide range of oblique incidence angles $\Psi(\varphi, \theta)$ [2]. A schematic of the so-called

harmonic ultrasonic backscatter polar scan (H-UBPS) method is shown in Figure 1a, in which the ultrasonic transducer is operated as both emitter and receiver. A H-UBPS experiment, recorded at $f=6$ MHz, is displayed in Figure 1b for a polycarbonate plate in which a perfect 2D surface corrugation with a depth of $17\ \mu\text{m}$ is ablated by means of a high-quality excimer laser [2]. The angular axis represents the in-plane orientation angle, further called the polar angle θ , the radial axis the angle with the vertical normal, further called the incident angle ϕ , while the assigned color pigment is a measure for the backscattered amplitude. Both the periodicities and symmetries of the insonified 2D surface structure are encoded in the exact location of the backscatter spikes (spikes 'A', 'B', 'BB', 'A+B' and 'A-B') in the H-UBPS experiment [2]. The reflected signal at normal incidence (spike 'O') is used to compensate for angular misalignment, thus experimental alignment is of minor concern.

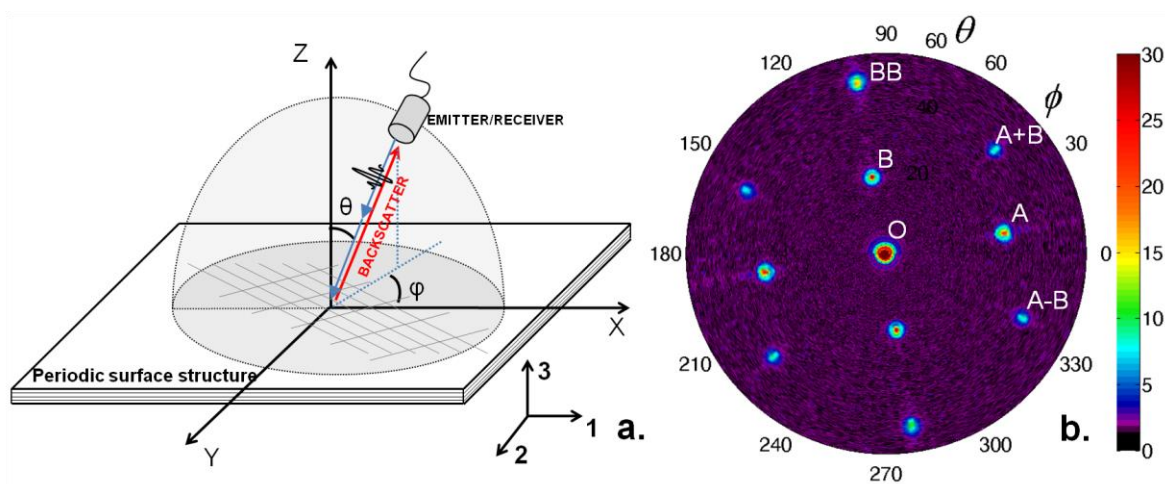


Figure 1: Schematic of the H-UBPS method (a) and H-UBPS recording ($f = 6$ MHz) for a 2D corrugated polycarbonate sample (b).

In this paper, we present an ultrasonic strain gauge which is based on the detection of shifting diffraction peaks in a H-UBPS image for measuring the in-plane strain field components. Additional analysis of the reflected signal at normal incidence on the other hand provides a measure for the out-of-plane strain component. As such, the ultrasonic strain gauge determines a 3D strain field. A limited physical background about the ultrasonic strain gauge is given in the next section. Section 3 provides several results obtained with the here introduced method for DC06 steel sheet at various strain levels. At last, several conclusions are rephrased in section 4.

2 BACKGROUND OF ULTRASONIC STRAIN GAUGE (USG)

2.1 In-plane Strain Field

The necessary condition for the appearance of diffraction spikes in a H-UBPS experiment is obviously the presence of a geometrical surface structure. Instead of manufacturing a specific surface corrugation which introduces residual stress concentrations and thus effectively weakens the material, we directly employ the deterministic surface roughness typically left during the manufacturing process of different materials. For example the skin passing of textured work rolls in case of a cold-rolled steel sheet or the imprint left by the peel-ply during a pressurized autoclave cycle for manufacturing fiber reinforced plastics. Figure 2a displays an optical image (coherence correlation interferometry) of the structured surface roughness ($R_a = 1.1\ \mu\text{m}$) of a cold-rolled DC06 steel sample. Figure 2b shows the obtained H-UBPS image at frequency $f=5$ MHz. The location of

the high amplitude back-diffraction spikes comprises information about the geometry of the local surface structure [1-2]. Appropriate analysis then yields the deterministic surface parameters, i.e. periodicities and orientations.

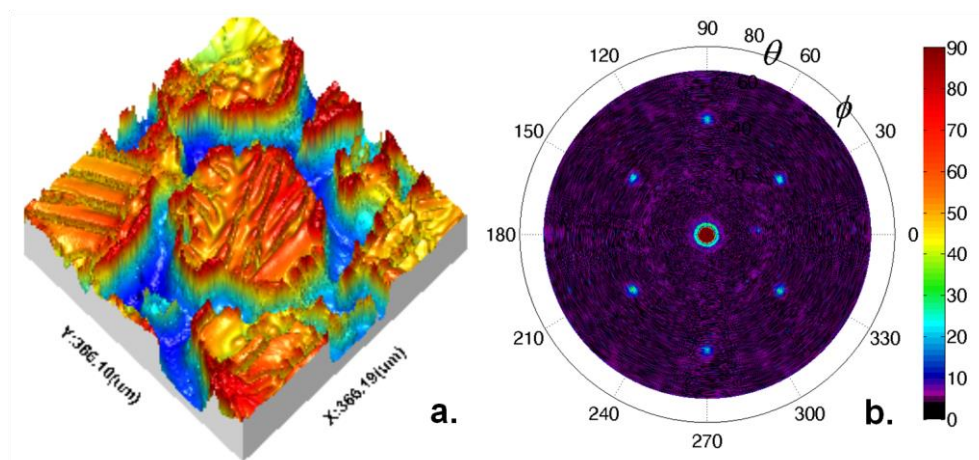


Figure 2: Unit cell of the surface structure of a cold-rolled DC06 steel sample (a) and H-UBPS recording at $f = 5$ MHz for an unstrained DC06 sample (b).

Upon loading the DC06 steel sheet, strain is induced which obviously transforms the surface structure parameters. As a consequence, a positional shift of the diffraction spikes in the H-UBPS image is induced (see Figure 3), reflecting the transformation of the surface parameters. Knowledge of both the original surface parameters and the transformed surface parameters then provides a means for determining the in-plane strain field components ϵ_{xx} and ϵ_{yy} at the surface.

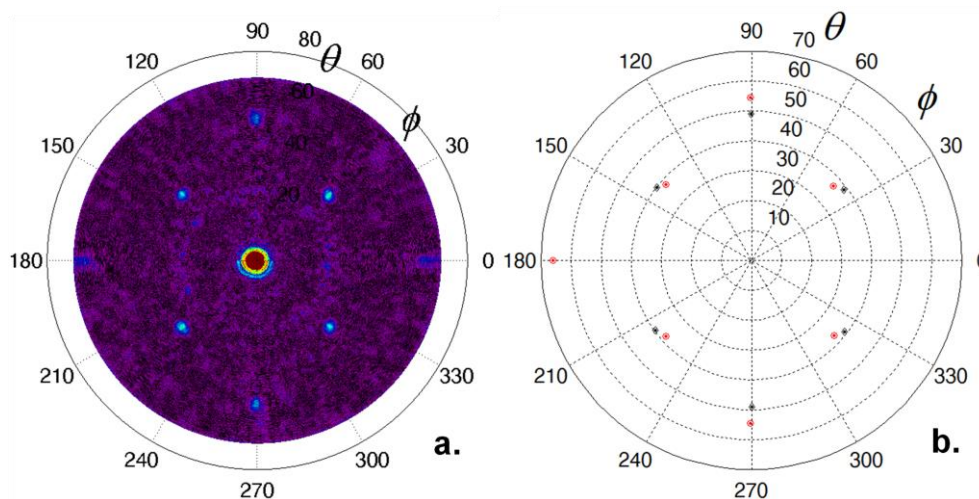


Figure 3: H-UBPS recording at $f = 5$ MHz for a strained DC06 sample (a) and extracted diffraction spikes for the unstrained (black) and strained (red) DC06 sample (b).

2.2 Out-of-plane Strain Field

By extending the H-UBPS methodology with the analysis of the reflected ultrasonic broadband pulse at normal incidence (which can be readily identified in the H-UBPS experiment) in temporal frequency domain, the stimulation conditions for a thickness resonance are exposed. This is numerically demonstrated in Figure 4 for the DC06 steel sheet. The considered material parameters

for the DC06 steel have been obtained through inversion of ultrasonic data [3]. Figure 4a displays the dispersion curves $\theta(fd)$ which put on view the Lamb wave stimulation conditions for plane wave insonification. The curves show the presence of several cut-off frequency-thicknesses fd at normal incidence $\theta = 0^\circ$ (indicated by the dashed lines) [4]. Figure 4b shows the computed reflection and transmission coefficient at normal incidence $\theta = 0^\circ$ as a function of frequency-thickness fd . At a cut-off frequency-thickness fd , it can be observed that the reflection and the transmission coefficient is characterized by a dip and a peak respectively. Hence, any shift of a cut-off frequency thickness fd has to be linked to a change in thickness d , thus providing a measure for the out-of-plane strain component ε_{zz} .

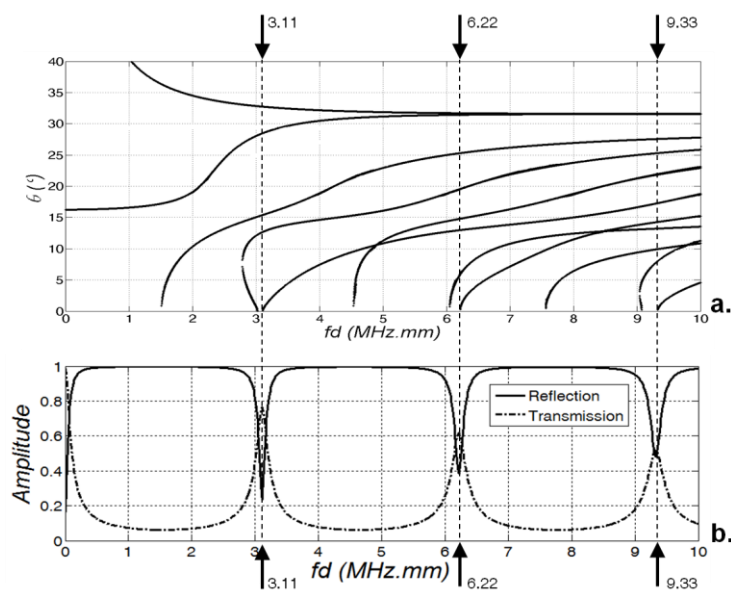


Figure 4: Dispersion curves $\theta(fd)$ (a) and reflection and transmission characteristics at $\theta = 0^\circ$ (b) for water-immersed DC06 steel. The thickness resonances are indicated by the dashed lines.

As such, the here presented ultrasonic strain gauge (USG) provides a non-contact and single-sided measurement of a local strain field (both the in-plane and the out-of-plane engineering strain components) without the necessity of difficult alignment procedures. Obviously, the local character of the strain measurement depends on the dimensions of the employed ultrasonic transducer.

3 EXPERIMENTAL APPROACH AND RESULTS

Results are presented for the widespread cold-rolled DC06 deep drawing steel having a designed thickness of $d = 0.8$ mm. First, the virgin DC06 steel sheet has been ultrasonically scanned at several arbitrary spots in order to obtain a measure of its original state, i.e. its deterministic surface roughness and its thickness. The employed transducer has a diameter of 13 mm and is operated in both the harmonic regime (in-plane parameters) and the pulsed regime (out-of-plane parameters). These scans indicate the highly uniform nature of the different geometrical parameters of the cold-rolled DC06 sheet. This is comfortable as we can take fixed reference values for all DC06 coupons rolled by these work rolls. Secondly, coupons have been cut at a length of 300 mm and a width of 30 mm which were then loaded in the plastic regime on an electromechanical Instron 5800R machine with 50 kN load cell. Plastic strains ranging from 2% up to 35% are considered. During the tensile tests, conventional strain measurement techniques have been applied, including manual micrometer (MM), longitudinal and transverse extensometer (EM) and mono- and stereovision digital image correlation (DIC). A typical stress strain curve obtained by extensometer and DIC is

presented in Figure 5a for specimen DC07-07 which was loaded up to a longitudinal plastic strain of $\sim 30\%$. Figure 5b-c shows the stereovision DIC results (transverse and longitudinal strain component) after unloading of the specimen (see red arrow in Figure 5a), and reveals a small degree of non-uniformity of the strain field.

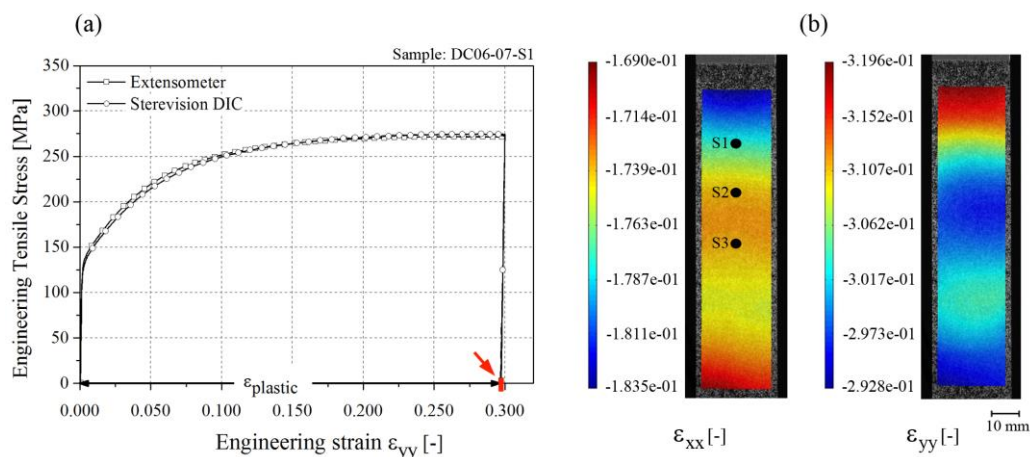


Figure 5: Stress-strain curve of specimen DC06-07 (a). Results of stereovision DIC: transverse strain component (b) and longitudinal strain component (c) for specimen DC06-07.

Because of the immobility of the ultrasound setup, the tested samples have to be first unloaded and demounted from the tensile machine before it can be placed in the ultrasound setup to perform a second scan. The immobility of the present ultrasound setup is the main reason why only plastic strain fields are considered in this study. The two ultrasound scans are then used to track down any change in the geometrical parameters of the DC06 specimen, in view of determining both the in-plane and the out-of-plane strain field. In the next, we discuss the obtained results for the DC06-07 specimen using the different strain gauge techniques more into detail.

The MM measurements have been obtained at the three different spots S_1 , S_2 and S_3 (see indicators at Figure 5b). For each spot, 10 measurements have been obtained from which an average value and a standard deviation is obtained. Obviously, the MM is limited to the extraction of the transverse and the out-of-plane strain component. The obtained results are listed in the first row of Table 1. The strong inequality of the ε_{yy} and ε_{zz} component indicates the plastic anisotropic nature of the tested DC06 steel sheet. A measure for quantifying the plastic anisotropy is found in the Lankford parameter R , which is the ratio between the transverse plastic strain component and the through-the-thickness plastic strain component [5]. Hence, a material which is plastically isotropic has a Lankford parameter $R = 1$. For the different spots of the DC06-07 specimen, we obtain a Lankford parameter $R_1 = 2.62$, $R_2 = 2.64$ and $R_3 = 2.73$, indicating its anisotropic plastic nature.

The EM provides only a single measurement of the in-plane strain field components at a single spot. This spot furthermore differs from the three above spots as the EM sensors have to be attached outside the DIC imaging field to avoid overlapping of the DIC speckle pattern. Thus, straightforward comparison with the strain results for spots S_1 , S_2 and S_3 has to be done with caution. In addition, the transverse strain measurement saturated at 8.33% for the DC06-07 specimen because the travel of the transverse extensometer is limited to ± 2.5 mm. The obtained EM result is listed in the second row of Table 1. To indicate that the longitudinal strain component was extracted at a different spot while the transverse strain component saturated, the row is put in gray.

The mono- and stereovision DIC results extracted at the different spots S_1 , S_2 and S_3 are listed in the third, respectively fourth row of Table 1. The differences between mono- and stereovision

data can be attributed to the fact that out-of-plane displacements are present coming from Poisson's contractions and deviations from the ideal planarity. It can be observed that the different DIC values compare well to both the MM data and the EM data.

Finally, the strain field at the three different spots S_1 , S_2 and S_3 has been measured by means of the newly developed ultrasonic strain gauge. Each spot has been scanned four times, from which an average value and a standard deviation is obtained. The results are listed in the fifth column of Table 1. Contrary to the other methods, the USG provides all three strain components. As a matter of fact, the USG also provides the in-plane shear strain component γ_{xy} . Though, for the here considered loading case (tension) this strain component has a negligible value and is therefore not discussed. It can be readily seen that the USG extracted values show good correspondence with the results obtained by means of the other methods, while the determined standard deviations are rather low. Though, the longitudinal strain component ε_{xx} for spot S_1 shows a clear divergence from the other results, which is easily explained on the basis of Figure 5c. Indeed, it can be observed that the longitudinal strain component ε_{xx} around the location of spot S_1 varies significantly. If the ultrasonic measurement at spot S_1 has been accidentally obtained 5 mm upwards, a value of $\sim 32\%$ would have been determined by means of DIC. Similar as done for the MM measurements, one can extract the Lankford ratios for the ultrasonic data at the different spots; $R_1 = 2.69$, $R_2 = 2.70$ and $R_3 = 2.71$ is obtained. Good correspondence with the above determined Lankford parameters is obtained. The consistency of the Lankford parameter is a clear indicator of the robustness and correctness of the determined strain fields.

Table 1: Strain field measurements (average values and standard deviation) for the three different spots of sample DC06-07. MM = micrometer, EM = extensometer, 2D/3D DIC = mono-/stereovision digital image correlation and USG = ultrasonic strain gauge. The EM row is put in gray because the data is obtained at a different spot, while the signal in the y -direction saturated.

	S_1			S_2			S_3		
	ε_{xx} (%)	ε_{yy} (%)	ε_{zz} (%)	ε_{xx} (%)	ε_{yy} (%)	ε_{zz} (%)	ε_{xx} (%)	ε_{yy} (%)	ε_{zz} (%)
MM	--	-17.022 ± 0.094	-6.501 ± 0.220	--	-16.575 ± 0.057	-6.272 ± 0.135	--	-16.711 ± 0.082	-6.120 ± 0.094
ME	29.672 --	-8.33 --	-- --	29.672 --	-8.33 --	-- --	29.672 --	-8.33 --	-- --
2D DIC	30.585 --	-17.491 --	-- --	29.981 --	-17.274 --	-- --	29.595 --	-17.101 --	-- --
3D DIC	30.158 --	-17.523 --	-- --	29.740 --	-17.212 --	-- --	29.352 --	-17.012 --	-- --
USG	32.350 ± 0.160	-17.808 ± 0.136	-6.609 ± 0.274	30.320 ± 0.131	-16.800 ± 0.183	-6.221 ± 0.112	30.443 ± 0.137	-17.158 ± 0.234	-6.338 ± 0.194

The above analysis is obviously valid for different applied loads and strain levels. For brevity however, we only show the MM and USG extracted Lankford ratios as a function of applied longitudinal strain (see Figure 6a). Note that the MM does not provide information about the longitudinal strain component, therefore the ultrasonic data has been adopted. Except for the data at $\varepsilon_{xx} = 2\%$, good agreement is found between both sets of data. The results further indicate a dependency of the Lankford parameter on the applied longitudinal strain. Such a dependency has recently been observed in literature for the DC06 steel [5].

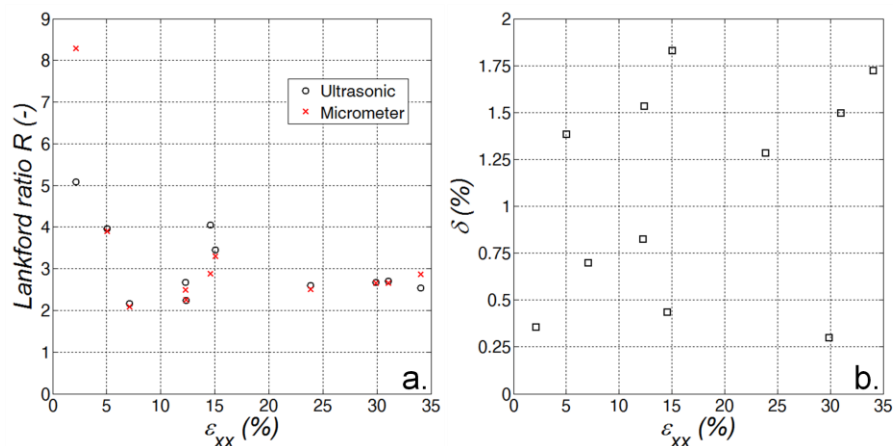


Figure 6: Lankford parameter R as a function of applied longitudinal strain ϵ_{xx} (a) and error δ on the incompressibility hypothesis (b).

The incompressibility hypothesis, which states that the volume remains constant upon straining a sample, provides another check for the accuracy and validity of the extracted strain field components. It has been found that the incompressibility hypothesis is not violated by more than $\delta = 1.8\%$ for the ultrasonic data (see Figure 6b). Unfortunately, this deviation cannot be compared with results of the other strain gauge techniques as none of them provide the three needed strain field components ϵ_{xx} , ϵ_{yy} and ϵ_{zz} .

CONCLUSION

A novel strain gauge method has been introduced on the basis of ultrasound waves. The in-plane strain field is measured by exploiting the interaction of oblique incident ultrasonic waves with a deterministic surface roughness, while the out-of-plane component is obtained by tracing the stimulation condition of a thickness resonance. The method has been applied to cold-rolled DC06 steel samples, which were loaded by means of a tensile machine to induce various plastic strain fields. The ultrasonic strain measurements have been validated with conventional strain gauge techniques, such as manual micrometer, mechanical extensometer, and both mono- and stereovision digital image correlation. Good agreement has been obtained with respect to the different methodologies. To demonstrate the capability of the ultrasonic strain gauge, Lankford ratios have been extracted as a function of strain level, revealing the strain dependent plastic anisotropy of the DC06 steel.

REFERENCES

- [1] 1. Bragg, W.L., *The diffraction of short electromagnetic waves by a crystal*. Proc. Cambridge Phil. Soc., 1913. **17**: p. 43-57.
- [2] 2. Kersemans, M., et al., *Ultrasonic Characterization of Subsurface 2D Corrugation*. Journal of nondestructive evaluation, In Press DOI 10.1007/s10921-014-0239-7, 2014.
- [3] 3. Kersemans, M., et al., *Identification of the elastic properties of isotropic and orthotropic thin-plate materials with the pulsed ultrasonic polar scan*. Experimental Mechanics, 2014. **IN Press DOI: 10.1007/s11340-014-9861-7**.
- [4] 4. Rose, J.L., *Ultrasonic Waves in Solid Media*. 1999: Cambridge University Press. 454.
- [5] 5. Safaei, M., *Constitutive modelling of anisotropic sheet metals based on a non-associated flow rule*. Ghent University, Faculty of engineering sciences and architecture (Ghent), PhD thesis, 2013: p. 246.

[6]